Fungal Genetics and Biology 144 (2020) 103466

Contents lists available at ScienceDirect

Fungal Genetics and Biology

journal homepage: www.elsevier.com/locate/yfgbi

Pseudoflowers produced by *Fusarium xyrophilum* on yellow-eyed grass (*Xyris* spp.) in Guyana: A novel floral mimicry system?

Imane Laraba [a,*], Susan P. McCormick [a], Martha M. Vaughan [a], Robert H. Proctor [a], Mark Busman [a], Michael Appell [a], Kerry O'Donnell [a], Frederick C. Felker [b], M. Catherine Aime [c], Kenneth J. Wurdack [d]

[a] *Mycotoxin Prevention and Applied Microbiology Research Unit, National Center for Agricultural Utilization Research, Agricultural Research Service, US Department of Agriculture, Peoria, IL 61604-3999, USA*
[b] *Functional Food Research Unit, National Center for Agricultural Utilization Research, Agricultural Research Service, US Department of Agriculture, Peoria, IL 61604-3999, USA*
[c] *Department of Botany and Plant Pathology, Purdue University, West Lafayette, IN 47907-2054, USA*
[d] *Department of Botany, National Museum of Natural History, Smithsonian Institution, Washington, DC 20013-2012, USA*

ARTICLE INFO

Keywords:
Floral mimics
Mating type
Pathogen
Pollinators
Systemic infection
Volatiles

ABSTRACT

Pseudoflower formation is arguably the rarest outcome of a plant-fungus interaction. Here we report on a novel putative floral mimicry system in which the pseudoflowers are composed entirely of fungal tissues in contrast to modified leaves documented in previous mimicry systems. Pseudoflowers on two perennial *Xyris* species (yellow-eyed grass, *X. setigera* and *X. surinamensis*) collected from savannas in Guyana were produced by *Fusarium xyrophilum*, a novel *Fusarium* species. These pseudoflowers mimic *Xyris* flowers in gross morphology and are ultraviolet reflective. Axenic cultures of *F. xyrophilum* produced two pigments that had fluorescence emission maxima in light ranges that trichromatic insects are sensitive to and volatiles known to attract insect pollinators. One of the volatiles emitted by *F. xyrophilum* cultures (i.e., 2-ethylhexanol) was also detected in the head space of *X. laxifolia* var. *iridifolia* flowers, a perennial species native to the New World. Results of microscopic and PCR analyses, combined with examination of gross morphology of the pseudoflowers, provide evidence that the fungus had established a systemic infection in both *Xyris* species, sterilized them and formed fungal pseudoflowers containing both mating type idiomorphs. *Fusarium xyrophilum* cultures also produced the auxin indole-3-acetic acid (IAA) and the cytokinin isopentenyl adenosine (iPR). Field observations revealed that pseudoflowers and *Xyris* flowers were both visited by bees. Together, the results suggest that *F. xyrophilum* pseudoflowers are a novel floral mimicry system that attracts insect pollinators, via visual and olfactory cues, into vectoring its conidia, which might facilitate outcrossing of this putatively heterothallic fungus and infection of previously uninfected plants.

1. Introduction

There are approximately 300,000 known angiosperm species and an estimated 2.2–3.8 million fungal species in the world (Hawksworth and Lücking, 2017; Sauquet et al., 2017). Many interactions between these two groups of organisms result in plant diseases, which are manifested by diverse symptoms. Pseudoflowers are arguably the rarest outcome of plant-fungus interactions. Induction of pseudoflowers has been documented in only a few species of rust fungi (Roy, 1993; Raguso and Roy, 1998; Pfunder and Roy, 2000; Naef et al., 2002) and in *Monilinia vaccinii-corymbosi* (*Mvc*), the mummy berry pathogen of blueberry (Batra and Batra, 1985). These pseudoflower-inducing fungi depend on insects to vector their spores to new hosts to complete their life cycle (Batra and Batra, 1985; Roy, 1993; Raguso and Roy, 1998; Naef et al., 2002). Pseudoflowers mimic host floral traits, thereby deceiving pollinators that facilitate transmission of infective spores or sexual outcrossing in heterothallic species (Ngugi and Scherm, 2006 and references therein). Pseudoflowers attract pollinators by visual floral mimicry that can

* Corresponding author at: Mycotoxin Prevention and Applied Microbiology Research Unit, National Center for Agricultural Utilization Research, Agricultural Research Service, US Department of Agriculture, 1815 North University Street, Peoria, IL 61604-3999, USA.
E-mail address: imane.laraba@usda.gov (I. Laraba).

https://doi.org/10.1016/j.fgb.2020.103466
Received 5 May 2020; Received in revised form 10 September 2020; Accepted 11 September 2020
Available online 19 September 2020

include ultraviolet (UV) reflectivity (Batra and Batra, 1985), by emitting distinctive floral fragrances (Raguso and Roy, 1998; McArt et al., 2016), and/or by producing a nectar-like reward (Roy, 1993).

One of the most intensively investigated floral mimicry systems involving pseudoflowers is that of the rust *Puccinia monoica*, which infects *Boechera stricta* (Drummond's rockcress, Brassicaceae) (Roy, 1993). Gene expression profiling revealed that the fungus reprograms its host during infection (Cano et al., 2013). Instead of flowering, the host produces a rosette of flower-like leaves covered with yellow spermogonia bearing spermatia. These pseudoflowers produce a sugary fluid that attracts insects, which facilitate outcrossing of the fungus by bringing spores of the opposite mating types to the same pseudoflower (Roy, 1993). Similarly, *Mvc* infection of blueberry plants can induce pseudoflowers that are UV reflective, produce sugary matrixes, and emit floral volatiles, all of which mimic the properties of the host flowers. Deceived pollinators transmit *Mvc* spores from pseudoflowers to uninfected blueberry flowers (Shinners and Olson, 1996; McArt et al., 2016).

Fusarium is one of the most agriculturally important fungal genera, comprising over 300 phylogenetically distinct species distributed among 23 monophyletic species complexes and several monotypic lineages (O'Donnell et al., 2013; Summerell, 2019). This genus contains a plethora of economically destructive cosmopolitan plant pathogens that cause localized or systemic infections in important crops. In addition, numerous *Fusarium* species contaminate food and feed with a broad range of mycotoxins, while some species have evolved as nonpathogenic endophytes of plants (Lee et al., 2009; Lofgren et al., 2018). The spread of *Fusarium* from an infected to an uninfected host occurs via the spread of asexual conidia and sexual ascospores. In *Fusarium*, as in other fungi, sexual reproduction is governed by genes located at mating type (*MAT*) loci. In heterothallic species, mating type is controlled by a single locus in which strains possess either a *MAT1-1* or *MAT1-2* idiomorph (Yun et al., 2000).

Recently, we discovered and described a new species of *Fusarium* that produces pseudoflowers on two perennial *Xyris* species (yellow-eyed grass, Xyridaceae, Poales), *X. setigera* and *X. surinamensis*, in the upland savannas of western Guyana (Laraba et al., 2019). With 250+ species worldwide, *Xyris* is the largest of the five genera of Xyridaceae. It contains annual and perennial species of grass-like herbs, typically inhabiting open, high hydroperiod environments such as acidic boggy savannas, wetlands, or seasonally wet sites. They can be conspicuous ecosystem elements with multiple sympatric species that are separated by phenology and/or small differences in hydrology. The greatest species diversity of *Xyris* is in the tropics and subtropics, but their distribution also extends into temperate regions such as the eastern U.S. (Kral, 1966, 1988; Campbell, 2011 and references herein).

Molecular phylogenetic analyses of multilocus DNA sequence data generated from pseudoflowers on *X. setigera* and *X. surinamensis*, and single-spore cultures isolated from them, indicated these floral mimics were produced by a novel *Fusarium* species, *F. xyrophilum* (Laraba et al., 2019). The analyses resolved this species as sister to *F. pseudocircinatum* within the African clade of the *F. fujikuroi* species complex (FFSC). The focus of the present study was to advance our understanding of this unique putative mimicry system and provide a foundation for future investigations. Our specific objectives were to (1) determine whether pseudoflowers are UV reflective and whether pigments produced by *F. xyrophilum* have light emission spectra that overlap insect-attracting spectra; (2) determine whether *F. xyrophilum* can produce volatiles that are known insect attractants and compare them to floral volatiles of *X. laxifolia* var. *iridifolia*; (3) test the hypothesis that *F. xyrophilum* had established a systemic infection in its perennial hosts and determine whether the pseudoflowers were modified leaves as reported for all other known fungus-induced floral mimicry systems; (4) analyze the genetic architecture of *MAT* loci and screen pseudoflowers for mating type idiomorph; and (5) investigate the ability of *F. xyrophilum* to produce phytohormones that may play a role in the formation of pseudoflowers.

2. Materials and methods

2.1. Host collections and pseudoflowers

Xyris setigera and *X. surinamensis* plants (Kral, 1988) bearing bright yellow-orange pseudoflowers that mimic host flowers in gross morphology (Fig. 1) were collected during botanical fieldwork in the Cuyuni-Mazaruni region of western Guyana in July 2010 and May 2012. The ungrazed upland savannas where the pseudoflowers were discovered occur along the drainage of the upper Mazaruni River in the Pakaraima Mountains where they form a discontinuous mosaic of small patches of natural vegetation over acidic white sand soils and shallow sandstone outcrops, usually associated with scrub communities and surrounded by rainforest. These savannas are part of the Guiana Shield, a region rich in endemic biota that encompasses most of Guyana, Surinam, French Guiana, as well as part of northern Brazil, eastern Colombia, and southern Venezuela. Plants and pseudoflowers were dried in the field using silica gel and then stored at −20 °C in the Smithsonian Institution (Washington, DC, USA). To further characterize the geographic distribution of pseudoflowers we visually screened worldwide *Xyris* species for their presence in the herbarium collections at MO, NY, and US (encompassing >12000 specimens). Single-spore pure cultures of *F. xyrophilum* were obtained by culturing microconidia from the pseudoflowers on *X. setigera* and *X. surinamensis* collected in 2012 on 3% water agar with antibiotics (Laraba et al., 2019). Key isolates were accessioned in the ARS Culture Collection and the *Fusarium* Research Center where they are available for distribution upon request (Supplementary Table 1).

2.2. UV reflectance and pigment analysis

Whole silica gel-dried infected inflorescences of *Xyris* spp. were imaged at 365 nm with a Nikon D70 digital camera (Minato, Tokyo, Japan) fitted with a UV-transmitting Coastal Optics 60 mm f/4 UV–VIS-IR APO macro lens (Jenoptik, Jupiter, FL, USA) and a Baadar UV-filter (325–369 nm) to assess whether the pseudoflowers are UV reflective. To identify the yellow-orange pigment(s) produced by the fungus, which might be responsible for the putative UV reflectivity of pseudoflowers, *F. xyrophilum* NRRL 62721 (Supplementary Table 1) was grown on potato dextrose agar (PDA; Difco, Detroit, MI, USA) under an alternating 12 h dark/12 h near-UV black and white fluorescent light cycle at 25 °C. After 7 days growth, mycelia were scraped from the surface of the cultures and extracted twice with 20 ml of methanol. The extract was concentrated under reduced pressure and a stream of nitrogen. The concentrated extract was initially separated on a silica gel 70–230 mesh column (Sigma-Aldrich, St. Louis, MO, USA) eluted with dichloromethane:methanol (95:5). One yellow band and one orange band were collected and analyzed with gas chromatography-mass spectrometry (GC–MS) and liquid chromatography-mass spectrometry (LC-MS/MS). The yellow and orange fractions were each further purified on a Sephadex LH-20 column (Sigma-Aldrich) eluted with methanol. Finally, the orange fraction was separated into two components on a Sep-Pak C18 column (Waters, Milford, MA, USA) eluted with methanol/water mixtures, dried under a stream of nitrogen and the extracts were then analyzed via LC-MS/MS. GC–MS analysis was carried out on a 6890 gas chromatograph coupled to a HP-5MS column (30 m, 0.25 mm, 0.25 μm) and a 5973 mass detector (Agilent Technologies, Wilmington, DE, USA) (Laraba et al., 2017). Compound identification was based on GC–MS comparisons with a NIST 11 library. Compound identity was confirmed using authentic standards (Busman, 2017). LC-MS/MS analysis was performed using a Dionex Ultimate 3000 liquid chromatography system connected to a Q Exactive mass spectrometer (Thermo Fisher Scientific, Waltham, MA, USA). Extracts were separated on a C18 column (Kinetex XB-C18 50 × 2.1 mm; Phenomenex, Torrance, CA, USA) eluted with a methanol/water gradient (0.6 ml/min, 20–95% methanol over 5 min) followed by MS detection by positive-mode electrospray ionization.

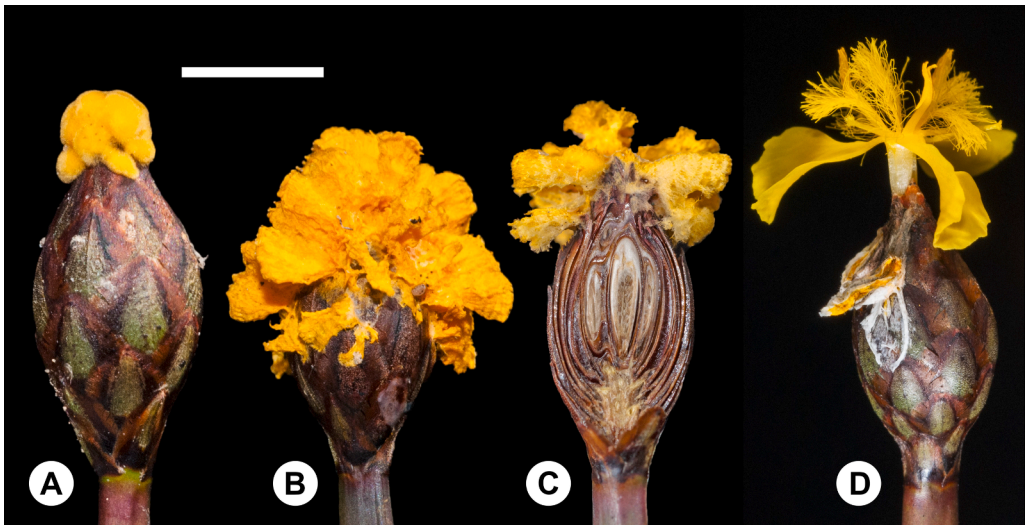

Fig. 1. Comparison of *Xyris* flower and *Fusarium xyrophilum* pseudoflowers collected in the Cuyuni-Mazaruni region of Guyana in 2010. (A) Young yellow-orange pseudoflower produced by *F. xyrophilum* emerging at tip of cone-like spike of *Xyris surinamensis*. (B) Mature pseudoflower of *F. xyrophilum* enveloping the entire *X. surinamensis* spike. (C) Longitudinal section of *X. surinamensis* spike showing partial fruit development in center and pseudoflower of *F. xyrophilum*. (D) Healthy yellow flower of *X. surinamensis* shown for comparison, with lateral petals and prominent erect hairlike staminodes. Scale bar: A–D = 5 mm. (For interpretation of the references to color in this figure legend, the reader is referred to the web version of this article.)

Compounds were identified by comparing ion mass, elution time, and ion fragmentation with a mass spectrometry library. To determine if the yellow-orange *F. xyrophilum* pseudoflowers contained the same pigment (s) detected in the culture extracts, pseudoflowers on *X. setigera* ($n = 6$) were extracted separately with 1 ml of methanol, acetone, and diethyl ether by vigorous shaking for 1 h. The three extracts were combined and then analyzed by LC-MS/MS as described above. The LC-MS/MS analyses identified two pigments from the orange extract. To determine whether the pigments produced by the fungus were UV reflective, the steady-state fluorescence emission spectra of the pigments were recorded within the 250–700 nm region on a Cary Eclipse fluorescence spectrophotometer (Agilent Technologies, Santa Clara, CA, USA) at room temperature (21–22 °C) using 10 × 10 mm quartz cells (Fisher Scientific, Pittsburgh, PA, USA) containing 3 ml of methanolic extracts of the pigments. The slit width for entrance and exit were set at 10 nm and scan rate was set at 120.0 nm/min with an average time of 0.5 s and 1 nm data intervals.

2.3. Characterization of volatiles emitted by F. xyrophilum cultures and X. laxifolia var. iridifolia flowers

Three strains of *F. xyrophilum* (NRRL 62710, 62721, and 66890; Supplementary Table 1) were grown in duplicate on V8 juice agar (Stevens, 1974) under an alternating 12 h dark/12 h near-UV black and white fluorescent light cycle at 25 °C. After a 7-day incubation period, single cultures on 100 mm × 15 mm V8 juice agar Petri plates and two sterile V8 agar plates were placed separately inside a 3 l glass desiccator that was sealed, and volatiles were collected from the head space using a closed-loop stripping method (Tholl et al., 2006). An air pump was inserted through the top of each jar and set to 4 V, which resulted in the recirculation of 3–4 volumes of air each hour. As air passed through the pump, volatiles were collected on a filter containing 25 mg of Porapak™ Porous Polymer adsorbent, type Q, 80–100 mesh (Supelco, Bellefonte, PA, USA) for 24 h. The compounds were then extracted from the adsorbent with 150 µl of dichloromethane and analyzed via GC–MS. GC–MS analysis of the trapped volatiles was performed on an Agilent 6890 chromatograph fitted with a HP-5MS column connected to an Agilent 5973 mass spectrometer. Samples were introduced with splitless injection at 50 °C, held at this temperature for 3 min, and then the column was heated to 250 °C at 30 °C/min where it was held for 1 min. Individual peaks were identified based on comparison of ion fragmentation patterns with a NIST 11 library. To confirm the identity of the compounds detected, they were compared to authentic standards purchased from Sigma-Aldrich except for nerolidol, which was purchased from the California Corporation for Biochemical Research (Los Angeles, CA, USA).

Since we did not have living material of the hosts for laboratory work, volatiles were analyzed from *X. laxifolia* var. *iridifolia* flowers collected in Carteret Co., North Carolina, U.S. (N34°43′5.43″, W76°58′0.79″) on 9 August 2020. This perennial species has similar morphology and savanna ecology as the hosts and we believe can serve as a good proxy for them. Plants were shipped overnight to Peoria, IL where they were potted in a mixture of sphagnum peat moss and perlite (2:1). The plants were then maintained at NCAUR in a controlled growth chamber with a 14 h photoperiod at 25 °C day/23 °C night, 50% relative humidity, and 650 µmol/s/m^2 photosynthetic photon flux density. Two sets of seven flowers were excised with part of the stem and placed in a beaker containing water inside a 3 l glass desiccator. Volatiles were then collected from them for 48 h using a closed-loop stripping method (Tholl et al., 2006). Compounds were extracted and analyzed via GC–MS as described above and identified based on comparison of ion fragmentation patterns with a NIST 11 library.

2.4. Systemic infection of Xyris spp. by F. xyrophilum

Microscopic and PCR analyses were conducted to assess whether *F. xyrophilum* established a systemic infection in both *Xyris* species. For scanning electron microscopy (SEM) silica gel-dried pseudoflowers from *X. surinamensis* and *X. setigera* were rehydrated in ultrapure water for 24 h at 25 °C, dehydrated in a graded ethanol series, freeze-fractured in liquid nitrogen with a single-edge razor blade (Zhou et al., 2018), and dried in a Samdri-PVT-3D critical point dryer (Tousimis, Rockville, MD, USA). Silica gel-dried scapes were sectioned by hand with a single-edge razor blade. Sections of the pseudoflowers and scapes were then mounted on SEM stubs, coated with gold in a SPI sputter coater (Structure Probe, West Chester, PA, USA) and examined in a JEOL JSM-6010A SEM (Tokyo, Japan).

To assess whether the fungus had established a systemic infection, a PCR assay was designed to amplify fragments of the ribosomal intergenic spacer region (IGS rDNA) of *F. xyrophilum* and the nuclear ribosomal small subunit (18S rDNA) of *Xyris*. PCR primer pair IGS-1f (5′-GCTGCTCAGTCTTGGTCG-3′) and IGS-1r (5′-CGCTTCCTGCCGGACAGG-3′) was used to amplify a 173-bp IGS rDNA fragment, and the plant specific primer pair Xy18-1f (5′-CATGCATGTGCAAGTATGAAC-3′) and Xy18-1r (5′-AATATACGCTATTGGAGCTGG-3′) was used to amplify a 558-bp 18S rDNA fragment. The PCR template was genomic DNA prepared from roots, scapes and pseudoflowers of *X. setigera* and *X. surinamensis* using a ZR Fungal/Bacterial DNA MiniPrep kit (Zymo Research, Irvine, CA, USA).

Genomic DNA extracted from axenic culture of NRRL 62721, the holotype of *F. xyrophilum* (Supplementary Table 1), and sterile ultrapure water were used as a positive control and no DNA negative control, respectively. Uniplex PCR reactions were performed in a total volume of 27.5 µl with 20 µl of Platinum PCR SuperMix High Fidelity (Invitrogen, Carlsbad, CA, USA), 2.5 µl of each primer (10 pmol/µl), and 2.5 µl of template DNA. The PCR was conducted in an Applied Biosystems 9700 thermocycler (ABI; Emeryville, CA, USA) using the following program: an initial denaturation at 94 °C for 2 min, followed by 30 cycles consisting of 30 s at 94 °C, 30 s at 55 °C, 3 min at 68 °C, a final elongation at 68 °C for 5 min, and a 4 °C soak. Amplification products and a 100 bp DNA ladder (Bio-Rad, Hercules, CA, USA) were separated by electrophoresis in a 2% agarose gel in 1 × TAE buffer pH 8.0 (40 mM Tris, 20 mM acetic acid, 1 mM EDTA) for 45 min. Afterwards the gel was stained with ethidium bromide and photographed using a Gel Doc EZ Imager (Bio-Rad). IGS rDNA and 18S rDNA amplicons were Sanger sequenced on an ABI 3730 Genetic Analyzer using PCR primers to confirm their identity as previously described (O'Donnell et al., 2010). Sequence chromatograms were edited using Sequencher 5.2.4 (Gene Codes Corp., Ann Arbor, MI, USA) and then used to query NCBI GenBank. The 7 IGS rDNA sequences were then aligned with a 40-strain IGS rDNA data set representing 35 species within the FFSC that included 6 reference strains of *F. xyrophilum* and an outgroup sequence of *F. oxysporum* NRRL 20433 using MUSCLE (Edgar, 2004) in SeaView 4.7 (Gouy et al., 2010). A phylogeny was then inferred using maximum likelihood as implemented in IQ-TREE 1.6.12 (Nguyen et al., 2015). IGS rDNA and 18S rDNA sequences generated were deposited in GenBank (accession numbers: MT919898–MT919944 and MT912635–MT912640).

2.5. Genetic architecture of mating type idiomorphs and screening of pseudoflowers for mating type idiomorph

The whole genome sequences of *F. xyrophilum* NRRL 62710, 62721, and 66890 were generated in a previous study (Laraba et al., 2019). Total genomic DNA was prepared using a ZR Fungal/Bacterial DNA MiniPrep™ Kit for sequencing in a MiSeq instrument (Illumina, San Diego, California). An Illumina Nextera XT Kit was used to prepare DNA libraries with an average insert size of 300 bp. The sequence reads generated were processed, assembled, and screened for contamination against 84 bacterial genomes and Nextera adapter sequences prior to *de novo* assembly using CLC Genomics Workbench version 12 (CLC bio, Qiagen, Aarhus, Denmark). Whole genome sequences are available in GenBank under the following accessions: VYXA00000000, VYWZ00000000, and VYWY00000000. In order to analyze the genetic architecture of *MAT* loci the BLASTn application in CLC bio was used to search the genomes of *F. xyrophilum* NRRL 62710, 62721, and 66890 strains for nucleotide sequences of the apurinic endonuclease (*APN1*) and cytoskeleton assembly control protein (*SLA2*), which flank mating type (*MAT*) loci in *Fusarium* (Martin et al., 2011; Hughes et al., 2014). The queries used in the analysis were *APN1* and *SLA2* sequences from *F. sublunatum* NRRL 13384 (GenBank accessions MT294273–MT294274). The online version of the *de novo* gene prediction software AUGUSTUS (Stanke et al., 2004), with *F. graminearum* gene models, was then used to predict the *MAT* genes to determine the structural organization of the *MAT* loci in the three strains of *F. xyrophilum*. Sequences of genes in the two *MAT* loci, and their flanking genes *APN1* and *SLA2* were annotated and deposited in NCBI GenBank (accession numbers: MT876217–MT876219). The flower-like rosettes on *X. setigera* and *X. surinamensis* (n = 8) collected in 2012 were screened for *MAT* idiomorph using a published uniplex PCR assay (Kerényi et al., 2004). Based on the whole genome sequence analyses, *F. xyrophilum* NRRL 62721 and NRRL 62710 were used, respectively, as positive controls for the *MAT1-1* and *MAT1-2* idiomorphs.

2.6. Phytohormone gene expression and production

Analyses of *F. xyrophilum* genome sequences indicated the presence of the 2-gene loci required for production of auxin and cytokinin phytohormones (Laraba et al., 2019). Based on this finding, NRRL 62710, 62721, and 66890 strains were examined for expression of auxin and cytokinin biosynthetic genes in liquid culture. Strains were grown separately in 25 ml glucose-yeast-extract-peptone broth (GYEP; Miller and Greenhalgh, 1985) containing three different concentrations of L-tryptophan (100, 500, and 1000 µg/ml; Sigma-Aldrich) in the dark on a rotary shaker set at 200 rpm and 28 °C. After 72 h, mycelium was harvested by filtration, ground to a powder in liquid nitrogen, and then total RNA was extracted with Trizol® reagent (Thermo Fisher Scientific). Once extracted, RNA was purified using a RNeasy Plant Mini Kit (Qiagen, Hilden, Germany) according to the manufacturer's protocol. RNA was reverse-transcribed into cDNA using Superscript II (Invitrogen) following instructions supplied by the manufacturer. The cDNA was then used as template for PCR in an ABI 9700 thermocycler as previously described (Laraba et al., 2018), using the following program: 94 °C for 90 s, 40 cycles of 94 °C for 30 s, 55 °C for 30 s, and 68 °C for 30 s, followed by a final extension at 68 °C for 5 min and a 4 °C soak. Primer pairs were designed based on the coding sequences of tryptophan-2-monooxygenase (*IAAM*), indole-3-acetamide hydrolase (*IAAH*), isopentenyltransferase (*IPTLOG1*), and a putative cytochrome P450 monooxygenase (*P450-1*) mined from the whole genome of *F. xyrophilum* NRRL 62721 (Supplementary Table 2).

For the indole-3-acetic acid (IAA) analysis, *F. xyrophilum* NRRL 62710, 62721, and 66890 strains were inoculated separately in 25 ml GYEP broth containing the same concentrations of L-tryptophan used for analysis of gene expression. After incubation in the dark at 200 rpm and 28 °C for 5 days, the cultures were extracted with 25 ml dichloromethane by vigorous shaking for 30 s and then the two phases were separated by centrifugation at 4695 rcf for 5 min. The dichloromethane phase was then concentrated to 1 ml under a nitrogen stream, derivatized with trimethylsilyldiazomethane in hexanes (362832; Sigma-Aldrich) for 30 min, collected via vapor phase extraction (Schmelz et al., 2004), and then analyzed for IAA via chemical ionization-gas chromatography/mass spectrometry (CI-GC/MS) profiling (Schmelz et al., 2004; Huffaker et al., 2011; Dafoe et al., 2013). The CI-GC/MS analysis was performed on a 7890B gas chromatograph coupled to a 5977A MS (Agilent Technologies) run in chemical ionization mode with isobutane as the ionization gas. Compounds were separated on an Agilent Technologies DB-35MS column (30 m, 0.25 mm, 0.25 µm) held at 70 °C for 1 min after injection, followed by a programmed temperature gradient of 15 °C/1 min to 300 °C where it was held for 7 min. Helium was used as the carrier gas with a 0.7 ml/min flow. Identification and quantification of IAA were based on a deuterated indole-2,4,5,6,7-d_5-3-acetic acid (d_5-IAA; CDN Isotopes, Pointe-Claire, Quebec, Canada) internal standard spiked into each sample.

Strains for cytokinin analysis were grown in GYEP broth under the same conditions described above. After 5 days, 2 ml of each culture were extracted with 2 ml acetonitrile-water (86:14 vol/vol) and passed through 13 mm, 0.45 µm nylon Acrodisc syringe filters (Sigma-Aldrich). The extracts were then analyzed via LC-MS and LC-MS/MS using the same method describe above. Cytokinin identity was confirmed by comparison of elution time, mass, and MS/MS fragmentation with purified standards (Cayman Chemical, Ann Arbor, MI, USA). Quantitation was done by monitoring the [M + H] + ions for each compound: trans zeatin (tZ), m/z 220.1; trans zeatin riboside (tZR), m/z 352.2; isopentenyl adenine (iP), m/z 204.1; and isopentenyl adenosine (iPR), m/z 336.2.

3. Results

3.1. Host collections and pseudoflowers

Based on field observations in the study area, pseudoflowers were abundant on two perennial *Xyris* species (*X. setigera* and *X. surinamensis*; Fig. 1A–C), along with a single occurrence on perennial *X. bicephala* (see Laraba et al., 2019). Our herbarium survey documented pseudoflowers

on 34 plant collections (including vouchers for this study) spanning four *Xyris* species in the Guiana Shield region. Records for *X. setigera* and *X. surinamensis* extend outside of Guyana, and we uncovered similar pseudoflowers on *X. subglabrata*, a perennial species from Colombia and Venezuela that closely resembles *X. setigera* (Supplementary data 1). *Xyris* inflorescences consist of a long, thin scape capped by a short cone-like spike composed of a series of imbricate bracts through which one or two short-lived bright yellow flowers emerge per day (Fig. 1D; Kral, 1988; K. Wurdack personal observation). Although *Xyris* were abundant across the savanna landscape, pseudoflowers were patchy and typically present on multiple plants growing in a clump. Very rarely did a clump of plants contain both flowers and pseudoflowers. Other than bearing pseudoflowers, infected plants were asymptomatic and appeared identical to healthy plants. *Xyris setigera* formed larger clumps of slightly smaller-leaved (less stocky) plants than *X. surinamensis*, but otherwise the two hosts were observed in proximity and appeared very similar except in small technical differences (i.e., leaf width, shape of bracts and petal margins, filament length, and seed size and sculpture; Kral, 1988). The pseudoflowers formed on the two species were identical. Multiple other *Xyris* species (i.e., annual *X. uleana* var. *angustifolia*, *X. guianensis*; short-lived perennial *X. cyperoides*, *X. involucrata*, *X. subuniflora*; and perennial *X. lanulobractea*, *X. laxifolia* var. *laxifolia*) and other Xyridaceae (i.e., *Abolboda* spp.) were also in close proximity, but never observed with pseudoflowers. *Xyris* flowers do not produce nectar but attract pollinators with pollen rewards (Kral, 1988), and in the field site the host flowers usually lasted only a few hours before shriveling. In contrast to the ephemeral nature of *Xyris* flowers, the pseudoflowers, persisted for multiple days. Field observations totaling several hours revealed that flowers and pseudoflowers were both visited by small bees, which suggests the insects could vector conidia of *F. xyrophilum* in addition to *Xyris* pollen.

Pseudoflowers first emerged at the tip of the *Xyris* inflorescence as a discoid mass that later enlarged and became confluent with fungal growth that emerged from between the lower bracts (Fig. 1A and B). As they matured, pseudoflowers formed multiple petaloid structures. Pseudoflowers were initially yellow-orange; however, the color faded to a lighter yellow in the oldest pseudoflowers. Infected inflorescences appeared to be functionally sterilized by the fungal growth, although some differentiated floral tissues were evident inside the spikes (Fig. 1C). The visual similarity between the host flowers and fungal pseudoflowers was striking (Fig. 1B–D), although there were differences in form and hue (yellow for the flowers but yellow-orange for the

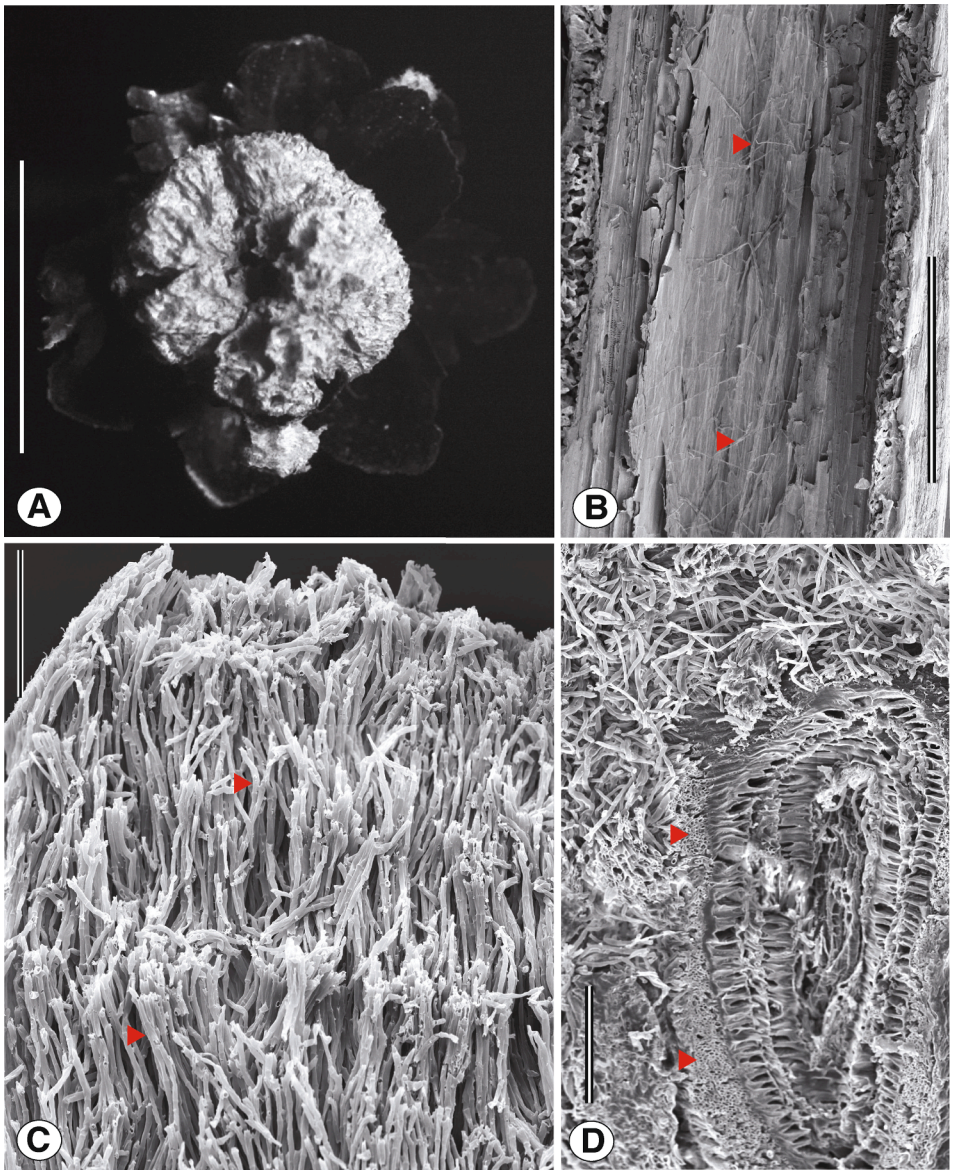

Fig. 2. Infection of *Xyris* spp. with *Fusarium xyrophilum*. (A) Ultraviolet reflective pseudoflower of *F. xyrophilum* on *Xyris surinamensis* imaged in UV light. (B) Scanning electron micrograph (SEM) showing mycelium (red arrowheads) growing on inner surface of median longitudinal section of *X. surinamensis* hollow scape. (C) SEM of cryofractured *F. xyrophilum* pseudoflower on *X. surinamensis* composed of textura intricata tissue (red arrowheads). (D) Cryofractured bract of *X. setigera* exposing vessel surrounded by textura prismatica tissue (red arrowheads) of *F. xyrophilum* (SEM). Scale bars: A = 5 mm; B = 0.5 mm; C–D = 100 μm. (For interpretation of the references to color in this figure legend, the reader is referred to the web version of this article.)

pseudoflowers).

3.2. UV reflectance and pigment analysis

UV imaging of infected inflorescences of *Xyris* at 365 nm revealed a strong visual contrast between dark bracts that were consistently UV absorbent and the bright UV reflective pseudoflowers (Fig. 2A). To determine whether *F. xyrophilum* pigments could be responsible for the UV reflectance of pseudoflowers, we used GC–MS and LC-MS/MS analyses to compare pigments present in solvent extracts of the pseudoflowers and pure cultures of the fungus. Pseudoflower extracts included one fraction (yellow fraction) that was similar in color to the pseudoflowers themselves. The most abundant metabolites detected in this fraction were 8-*O*-methylfusarubin and fatty acids. Extracts of pure cultures of *F. xyrophilum* included two fractions (yellow and orange fractions) that were similar in color to the pseudoflowers. Analysis of the orange fraction revealed the presence of two pigments, 8-*O*-methylfusarubin and 8-*O*-methylbostrycoidin, which are products of the fusarubin biosynthetic pathway (Studt et al., 2012). In contrast, fatty acids were the only metabolites detected in the yellow fraction of cultures.

Fluorescence emissions of the 8-*O*-methylfusarubin and 8-*O*-methylbostrycoidin pigments were recorded at different excitation wavelengths. The two pigments showed complex UV absorbance and fluorescence emission spectra in the visible range (400–750 nm; Fig. 3) together with emissions in the UV range (250–400 nm; Fig. 4). There were multiple excitation wavelengths (240, 260, 280, 340, and 395 nm) for 8-*O*-methylfusarubin that resulted in sharply peaked emission maxima in the visible range (Fig. 3A). Excitation of 8-*O*-methylfusarubin at 240 and 395 nm resulted in emission maxima in the blue light range: excitation with 240 nm resulted in a sharp emission peak at 486 nm, with complex shoulder peaks; whereas excitation with 395 nm resulted in a broad less intense emission peak at 450 nm. Sharp and intense emission maxima were also observed at 521 and 561 nm (green range) when the pigment was excited at 260 and 280 nm, respectively. 8-*O*-methylfusarubin also exhibited fluorescence emission at 680 nm (deep-red range) when excited at 340 nm. In addition, excitation of this pigment at 260, 280, and 340 nm also resulted in less intense and broad emission peaks (Fig. 3A; Supplementary Table 3). 8-*O*-methylbostrycoidin exhibited a less complex fluorescence emission profile between 400 and 700 nm (Fig. 3B). Excitation at 245, 267, and 325 nm resulted in sharp emission maxima at 495 nm (blue), 537 (green), and 650 nm (deep red), respectively. The later three excitation wavelengths also gave other less intense emission peaks (Fig. 3B; Supplementary Table 3). Interestingly, 8-*O*-methylfusarubin and 8-*O*-methylbostrycoidin also exhibited fluorescence emissions in the UV-A (315–400 nm) and UV-B (280–315 nm) when excited at 227 nm. 8-*O*-methylfusarubin and 8-*O*-methylbostrycoidin had the most intense UV emission peaks at 295 and 335 nm and less intense peaks at 325 and 300 nm respectively (Fig. 4).

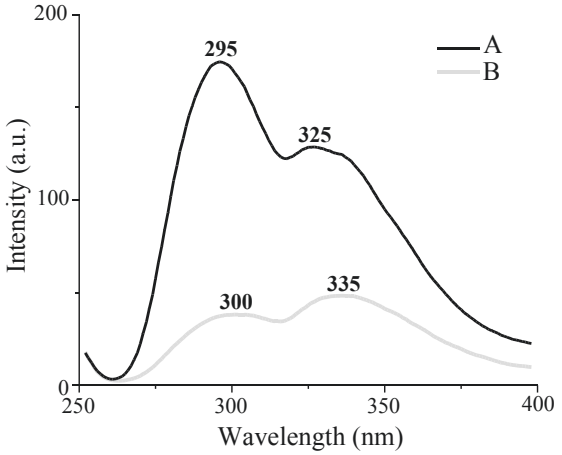

Fig. 4. Fluorescence emission spectra in UV between 250 and 400 nm of 8-*O*-methylfusarubin (A) and 8-*O*-methylbostrycoidin (B) extracted from *Fusarium xyrophilum* cultures. Excitation wavelength was 227 nm. a.u. is relative emission intensity.

3.3. Characterization of volatiles emitted by F. xyrophilum cultures and X. laxifolia var. iridifolia flowers

GC–MS analysis of duplicate cultures of *F. xyrophilum* NRRL 62710, 62721, and 66890 revealed that they emitted volatile compounds, including sesquiterpenoid, benzenoid, ester and fatty acid derivatives. Seven volatiles (isobutyl acetate, isoamyl acetate, phenylethyl acetate, 2-ethylhexanol, anthranilic acid, α-farnesene, and nerolidol) were identified in the head space of all *F. xyrophilum* cultures (Fig. 5). Three additional compounds (benzaldehyde, methyl anthranilate, and β-farnesene) were detected in the head space of only some *F. xyrophilum* cultures (Fig. 5; Supplementary Table 4). None of the ten volatile compounds was, however, detected in the head space of the sterile V8 agar negative control plates. GC–MS analysis of volatiles collected from two sets of *X. laxifolia* var. *iridifolia* flowers showed that they released 2-ethylhexanol, benzeneacetaldehyde, and several unidentified compounds (Supplementary Fig. S1). Of the 10 volatiles emitted by

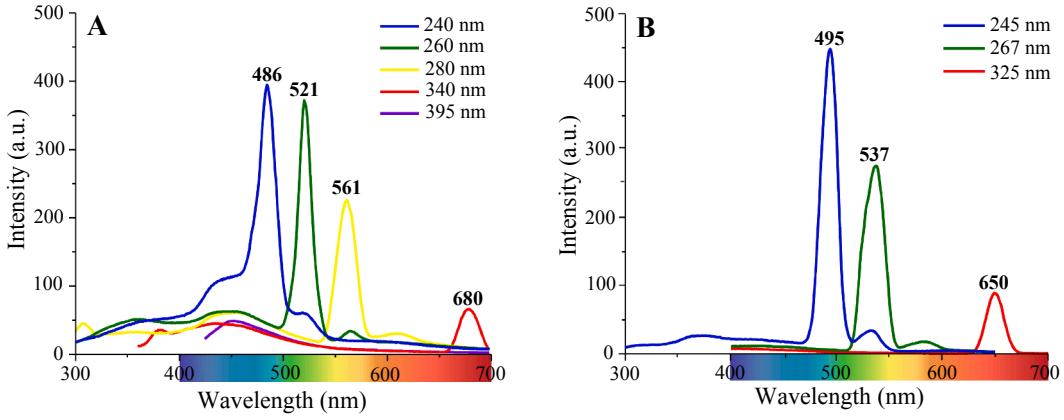

Fig. 3. Fluorescence emission spectra between 300 and 700 nm resulting from excitation of two pigments extracted from *Fusarium xyrophilum* cultures. (A) Fluorescence emission maxima for 8-*O*-methylfusarubin were 486, 521, 561, and 680 nm. (B) Emission maxima for 8-*O*-methylbostrycoidin were 495, 537, and 650 nm. a.u. is relative emission intensity. Each colored line shows emission data for a different excitation wavelength. A key indicating the excitation wavelength corresponding to each color is shown in the upper right corner of each figure.

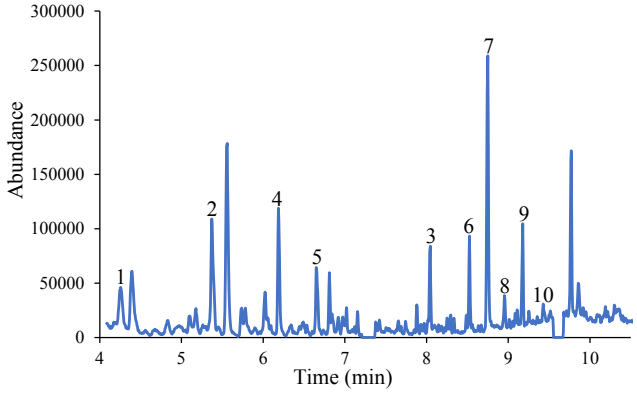

Fig. 5. GC–MS spectrum of volatiles emitted from *Fusarium xyrophilum* strains. 1. Isobutyl acetate. 2. Isoamyl acetate. 3. Phenylethyl acetate. 4. Benzaldehyde. 5. 2-ethylhexanol. 6. Methyl anthranilate. 7. Anthranilic acid. 8. β-farnesene. 9. α-farnesene. 10. Nerolidol.

F. xyrophilum cultures, 2-ethylhexanol was the only one produced by *X. laxifolia* var. *iridifolia*.

3.4. Systemic infection of Xyris spp. by F. xyrophilum

A medium longitudinal section of a *X. surinamensis* scape viewed via SEM revealed that a filamentous fungus had colonized the internal surface of the hollow scape (Fig. 2B). Pseudoflowers were composed of textura intricata (i.e., interwoven, irregularly arranged hyphae) and textura prismatica (i.e., anticlinallly arranged, densely packed hyphae) tissues (Kirk et al., 2008), some of which surrounded host vessel cells in the cone-like spike (Fig. 2C and D). Results of a PCR assay targeting the *F. xyrophilum* IGS rDNA confirmed the presence of the fungus in *X. setigera* and *X. surinamensis* roots, scapes and pseudoflowers (amplicon size = 173 bp; Fig. 6). IGS rDNA sequences generated from amplicons confirmed that the fungus was *F. xyrophilum* and distinguish it from all other fusaria in the FFSC (Supplementary Fig. S2). In addition, the no DNA negative control used indicated the PCR reaction mix was not contaminated with *Fusarium* DNA. The PCR assay targeting *Xyris* 18S rDNA yielded products with DNA from all three plant tissues of *X. setigera* and *X. surinamensis* (amplicon size = 558 bp; Fig. 6). BLASTn searches of NCBI GenBank using 18S rDNA sequences generated from the amplicons revealed that they exhibited the highest identity (99.8% and 98.9%, respectively, for *X. setigera* and *X. surinamensis*) to *X. difformis* AF168881, the only *Xyris* species available in GenBank.

3.5. Genetic architecture of mating type idiomorphs and screening of pseudoflowers for mating type idiomorph

The three *F. xyrophilum* genomes were subjected to BLASTn analysis using genes that flank the *MAT* loci in *Fusarium* (i.e., *APN1* and *SLA2*) as query sequences. The analysis revealed that NRRL 62710 and 66890 strains had the *MAT1-2* idiomorph, whereas NRRL 62721 strain had *MAT1-1* as previously reported in Laraba et al. (2019). Analysis of the *MAT* sequences with the *ab initio* prediction tool AUGUSTUS (Stanke et al., 2004) indicated that gene order, content and direction of translation of the three genes within *MAT1-1* and two genes within *MAT1-2* were identical to that reported for other members of the FFSC (Martin et al., 2011). A PCR assay for determining *MAT* idiomorph (Kerényi et al., 2004) revealed that *F. xyrophilum* pseudoflowers formed on *X. surinamensis* and *X. setigera* contained *MAT1-1* and *MAT1-2* idiomorphs.

3.6. Phytohormone gene expression and production

Expression of auxin and cytokinin biosynthetic genes in *F. xyrophilum*

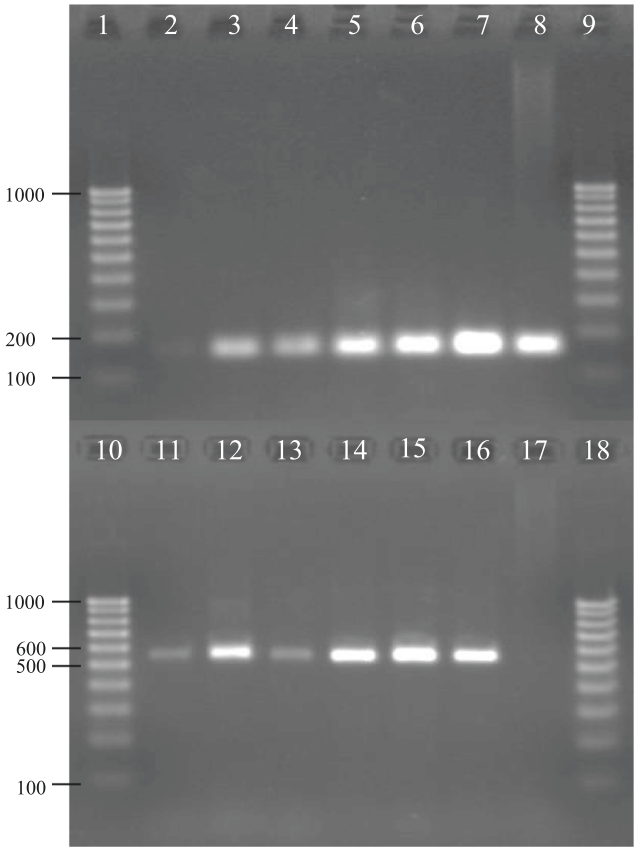

Fig. 6. PCR assay for *Fusarium xyrophilum* (lanes 2–8) and *Xyris* (lanes 11–16). Lanes 1, 9–10, 18. 100 bp DNA ladder. Lanes 2–4. *F. xyrophilum* detected in *X. surinamensis* roots (2), scapes (3), and pseudoflowers (4). Lanes 5–7. *F. xyrophilum* detected in *X. setigera* roots (5), scapes (6), and pseudoflowers (7). Lane 8. Positive control *F. xyrophilum* NRRL 62721. Lanes 11–13. *X. surinamensis* DNA detected in roots (11), scapes (12), and pseudoflowers (13). Lanes 14–16. *X. setigera* DNA detected in roots (14), scapes (15), and pseudoflowers (16). 17. Negative control (ultrapure water). The partial IGS rDNA amplicon of *F. xyrophilum* was 173 bp; the partial SSU (18S) rDNA amplicon of *X. setigera* and *X. surinamensis* was 558 bp.

NRRL 62710, 62721, and 66890 strains grown in liquid GYEP medium was examined by RT-PCR analysis. Expression of both auxin biosynthetic genes (*IAAM* and *IAAH*) and both cytokinin biosynthetic genes (*IPTLOG1* and *P450-1*) were detected in all three strains. These data provide evidence that the strains likely produced IAA and cytokinin under the culture conditions tested. To confirm IAA production, we conducted CI-GC/MS analysis of the GYEP culture extracts of the three strains. This analysis revealed that all three strains produced high levels of IAA (Fig. 7), and that production level was positively correlated with the concentration of L-tryptophan added to the culture medium (Table 1). To confirm cytokinin production, we analyzed filtrates of liquid GYEP cultures using LC-MS/MS. The analysis revealed that all three *F. xyrophilum* strains produced the cytokinin iPR (Fig. 8), albeit at low levels (NRRL 62710 = 2.55 ng/ml, NRRL 62721 = 2.53 ng/ml, and NRRL 66890 = 5.1 ng/ml). No other cytokinin analogs were detected under the conditions tested.

4. Discussion

4.1. Host collections and pseudoflowers

Here we further investigate a recently discovered putative floral mimicry system involving a novel species of *Fusarium*, *F. xyrophilum* (Laraba et al., 2019), which produces flower-like structures (i.e.,

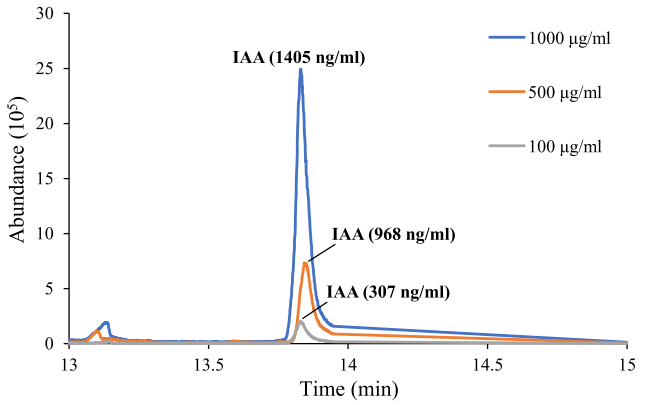

Fig. 7. Selective ion chromatogram for *m/z* 190 detecting IAA in liquid cultures of *Fusarium xyrophilum* NRRL 62721 supplemented with three concentrations of L-tryptophan (100, 500, 1000 µg/ml).

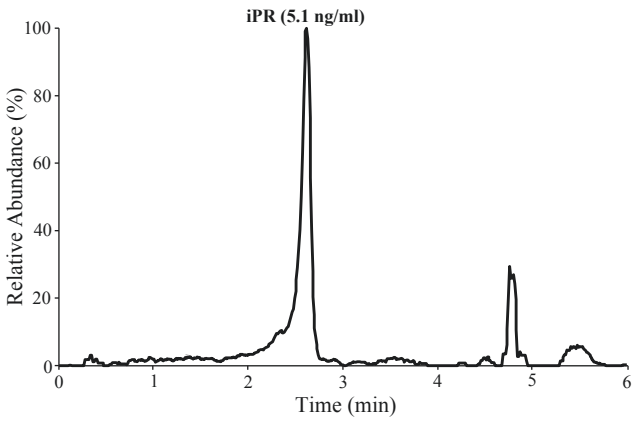

Fig. 8. LC-MS/MS spectrum of cytokinin iPR detected in liquid culture of *Fusarium xyrophilum* NRRL 66890.

Table 1
IAA production by *Fusarium xyrophilum* strains in GYEP broth.

NRRL no.[a]	L-tryptophan (µg/ml)[b]	IAA (ng/25 ml)[c]
	100	41
62710	500	247
	1000	549
	100	369
66890	500	373
	1000	1097
	100	307
62721	500	968
	1000	1405

[a] NRRL, strains of *F. xyrophilum* available from ARS Culture Collection, Peoria, IL.
[b] Concentrations of L-tryptophan supplemented in GYEP broth.
[c] Concentrations of IAA (indole-3-acetic acid) synthetized in GYEP broth.

pseudoflowers) on two perennial species of yellow-eyed grass (*Xyris* spp.) in Guyana. Although the study area contained multiple sympatric *Xyris* species, the perennial species *X. setigera* and *X. surinamensis* were the only plant species (except a single occurrence on *X. bicephala*) observed in the field with pseudoflowers, suggesting that *F. xyrophilum* might exhibit host preferences. Further support for host specificity is that our herbarium collection survey of worldwide *Xyris* diversity could identify only a single additional pseudoflower-possessing *Xyris* species (*X. suglabrata*) in addition to the known hosts (Supplementary data 1). We have not verified the fungus on *X. subglabrata* but speculate it is *F. xyrophilum* given the similar pseudoflower morphology and biogeography. *Fusarium xyrophilum* has only been reported from the Guiana Shield region and is the only known pseudoflower-producing *Fusarium* species. *Fusarium xyrophilum* pseudoflowers mimic *Xyris* flowers in color, shape and size. This system is unique because the entire pseudoflower is made up of fungal tissues, in contrast to the floral mimicry systems previously described for *Puccinia* (Roy, 1993; Naef et al., 2002), *Uromyces* (Pfunder and Roy, 2000), and *Monilinia* (Batra and Batra, 1985), where the floral mimics are modified host leaves that are covered with fungal spores and an insect-attracting nectar-like reward. We found that pseudoflowers and true *Xyris* flowers were visited by small bees, pseudoflowers were UV reflective, pigments produced by *F. xyrophilum* have fluorescence emission spectra that match the spectral sensitivity of insects with trichromatic color vision, and the fungus produced volatiles known to attract insect pollinators, including one volatile that was also detected in *Xyris* floral scent. Thus, our working hypothesis is that *F. xyrophilum* pseudoflowers are an adaptive floral mimicry system that includes production of visual and olfactory cues to attract pollinators who transfer conidia among pseudoflowers and to uninfected hosts. However, in order to determine whether this is a true mimicry system further field research is necessary to verify if mimics and *Xyris* flowers share the same insect visitors, investigate what, if any, visual and/or olfactory signals function as insect attractants in this system, and elucidate the evolutionary ecology and transmission biology of *F. xyrophilum* pseudoflowers. Although the *F. xyrophilum* infection of *Xyris* appears to be detrimental to the individual plants affected because normal floral development and reproduction are inhibited, field experiments are also needed to assess whether the long-lived pseudoflowers benefit the host by attracting more insect visitations to the ephemeral true flowers (Roy, 1996).

4.2. UV reflectance and pigment analysis

Pigmented flowers often possess UV patterns that are only visible to insect pollinators whose eyes possess UV photoreceptors (Eisner, 2002; Mazza et al., 2010). Batra and Batra (1985) discovered that pseudoflowers induced by *Mvc* on blueberries reflect UV light and therefore may provide a visual contrast similar to real flowers that attracts bees and flies who aid the fungus in completing the disease cycle by dispersing conidia. Bees and many other insects have a trichromatic color vision system, possessing UV, blue- and green-sensitive photoreceptors in their compound eyes (Ostroverkhova et al., 2018). Fluorescence emission spectra that were obtained for the 8-*O*-methylfusarubin and 8-*O*-methylbostrycoidin pigments produced by *F. xyrophilum* overlap with the trichromatic spectral sensitivity of diverse members of the order Hymenoptera, which includes bees, ants, sawflies, and wasps (Supplementary Fig. S3; Peitsch et al., 1992; Briscoe and Chittka, 2001). Interestingly, the peak emission maximum for both pigments was at the top end of the blue spectral region (486 and 495 nm), which corresponds precisely with the region that bees show the strongest attraction to (Rao and Ostroverkhova, 2015). These data provide evidence that at least two pigments are likely responsible for UV reflectance of the pseudoflowers. Although fluorescence emissions of the pigments in UV-A (315–400 nm) and UV-B ($\lambda \leq 315$ nm) were minor, the emission maxima of 295/325 nm for 8-*O*-methylfusarubin and 300/335 nm for 8-*O*-methylbostrycoidin correspond well with the maximum sensitivity of 290/330 nm wavelengths reported for thrips (Mazza et al., 2010). Accordingly, we speculate that pigments in *F. xyrophilum* serve as visual cues that attract pollinators with trichromatic color vision to pseudoflowers. In turn, duped pollinators might vector conidia of this self-sterile fungus to other flowers and pseudoflowers. In addition to detailed fieldwork to verify this hypothesis, UV reflectance patterns of *Xyris* inflorescences and fungal pseudoflowers need to be compared to determine if they are similar enough to lure insects.

4.3. Characterization of volatiles emitted by F. xyrophilum cultures and X. laxifolia var. iridifolia flowers

Olfactory cues involved in attracting flower-visiting insects have been characterized in several plant-pollinator systems where pollinators use plant volatiles to locate flowers (Haverkamp et al., 2018). Pseudoflowers induced by some fungi such as *Mvc* can also mimic host olfactory cues, thereby attracting pollinators (McArt et al., 2016). To understand the degree of mimicry in the present system, volatiles were collected from the head space of axenic cultures of *F. xyrophilum* to determine whether insect attractants were produced. This analysis revealed that *F. xyrophilum* emitted a blend of volatiles, most of which have been shown to possess insect attractant properties. Among the compounds released were three sesquiterpenoids (α-farnesene, nerolidol, and β-farnesene). α-farnesene, which is commonly found in floral volatile profiles, is one of the main compounds that bees use to locate nectar resources on several flowering plants (Blight et al., 1997; Twidle et al., 2015). Nerolidol was also previously reported as a major volatile in orange flower fragrances that are attractive to the stingless bee *Scaptotrigona pectoralis* (Grajales-Conesa et al., 2012). Although β-farnesene emitted by some *F. xyrophilum* cultures is not a common substance in floral scents, its biological activity was confirmed as part of a marking pheromone of bumble bees (Svensson and Bergström, 1977; Valterová et al., 2007) and this sesquiterpene was the major volatile produced by the orchid *Orchis pauciflora*, which is pollinated exclusively by bees (Valterová et al., 2007). Moreover, experiments conducted by Valterová et al. (2007) demonstrated that addition of *E*-β-farnesene to *O. pauciflora* inflorescences increased their attractiveness to *Bombus terrestris* (bumble bee) females. We also identified aromatic and ester-derivative volatiles (benzaldehyde, methyl anthranilate, isoamyl acetate, and phenylethyl acetate). Benzaldehyde is a common aromatic floral compound that was identified from uninfected *Arabis* vegetative tissues and pseudoflowers that were induced by *Puccinia* spp. (Raguso and Roy, 1998). It has also been reported in several lepidopteran pollination systems and appears to work synergistically with other benzenoids to attract *B. terrestris* workers (Andersson et al., 2002; El-Sayed et al., 2018). Similarly, phenylethyl acetate was previously reported to be produced by pseudoflowers on *Arabis* (Raguso and Roy, 1998) and to attract euglossine (orchid) bees (Hills et al., 1972). Methyl anthranilate, a benzoate ester of anthranilic acid, is also a well-known floral attractant of several hymenopterans, coleopterans, dipterans, and thrips (Murai et al., 2000; James, 2005). Lastly, isoamyl acetate, known as banana oil, is a powerful attractant for moths when combined with acetic acid (Landolt et al., 2011). Our finding that *F. xyrophilum* cultures emitted floral volatiles supports the interpretation that pseudoflowers might release volatiles that attract insects.

We compared floral and fungus volatiles for common signatures, using a *Xyris* species similar to the hosts. To our knowledge this is the first report of Xyridaceae floral scent profiles, and *Xyris* flowers have been typically described as odorless (Kral, 1966; K. Wurdack personal observation). Analysis of volatiles collected from *F. xyrophilum* cultures and *X. laxifolia* var. *iridifolia* flowers revealed that they both produce the semiochemical 2-ethylhexanol. This compound is released by numerous plants from diverse families including Fabaceae and Solanaceae (Jakobsen et al., 1995; Chen et al., 2017). Behavioral assays have revealed that this alcohol is a strong attractant for honey and bumble bees (Rering et al., 2018; Schaeffer et al., 2019), white flies (Chen et al., 2017), and the cowpea weevil (Ajayi et al., 2015). This finding supports the hypothesis that *F. xyrophilum* may be mimicking floral olfactory cues of the hosts, *X. setigera* and *X. surinamensis*. To verify this hypothesis, volatiles produced by pseudoflowers *in situ* need to be analyzed when expeditions to Guyana are possible to determine if they are similar to *X. setigera* and *X. surinamensis* floral scents so that their role in this system can be elucidated.

4.4. Systemic infection of Xyris spp. by F. xyrophilum

Pseudoflower-inducing fungi typically sterilize and overwinter in their host tissues, which are all perennials (Pfunder and Roy, 2000; McArt et al., 2016). SEM images of *Xyris* scapes and pseudoflowers and results of a PCR assay suggest that *F. xyrophilum* had established a systemic infection and produced pseudoflowers on two perennial *Xyris* spp. in Guyana. In addition, the infected plants we examined were all functionally sterilized, even if limited floral development was anatomically evident. While asymptomatic *X. setigera* and *X. surinamensis* plants (i.e., plants without pseudoflowers) were not available for study, it is reasonable to assume that *F. xyrophilum* might grow in them endophytically for a year or more before forming pseudoflowers on these perennial hosts.

In the absence of a robust species-level phylogeny for *Xyris*, it is unclear whether the association of *F. xyrophilum* with *X. setigera* and *X. surinamensis* is due to diversifying coevolution or a host jump based on geographic and ecological proximity (Roy, 2001). Elucidating the evolutionary history of this association promises to be a fertile avenue of research because the known distribution of these two hosts spans multiple countries in northern South America (Kral, 1988), and because at least 44 *Xyris* species are represented in the Guiana Shield region (Berry and Riina, 2005).

4.5. Genetic architecture of mating type idiomorphs and screening of pseudoflowers for mating type idiomorph

Whole genome analyses revealed that *F. xyrophilum* NRRL 62710 and 66890 had the *MAT1-2* idiomorph, whereas NRRL 62721 had *MAT1-1* as previously reported in Laraba et al. (2019). The same study using a PCR assay for *MAT* idiomorph determination revealed that 20*F. xyrophilum* strains derived from single conidia recovered from the pseudoflowers were either *MAT1-1* or *MAT1-2*, suggesting that if this fungus possesses a sexual cycle, it is heterothallic (Supplementary Table 1; Laraba et al., 2019). However, *MAT1-1* and *MAT1-2* strains of *F. xyrophilum* failed to cross and produce perithecia in vitro (Laraba et al., 2019). Analysis of the idiomorphs in *F. xyrophilum* indicate that the content, order, and direction of transcription of the three genes within *MAT1-1* and the two within *MAT1-2* is identical to that previously reported for other species in the FFSC (Martin et al., 2011). The discovery that pseudoflowers produced on *X. setigera* and *X. surinamensis* contained both idiomorphs fits the hypothesis that mating-compatible *MAT1-1* and *MAT1-2* strains might have been vectored to the same host by pollinators, such as pollen-collecting bees and syrphid flies, the main visitors of *Xyris* (Ramirez, 1993; Boyd et al., 2011). In this scenario, the duped insects would facilitate outcrossing of *F. xyrophilum*. Field studies are needed to determine whether *Xyris* flowers and pseudoflowers share the same insect visitors and whether they vector conidia. Behavioral assays are also necessary to determine if insects carrying fungal propagules fly between pseudoflowers and/or true flowers, which would facilitate transmission of infective spores and infections of healthy plants. Diamond et al. (2006) found that pollen-like conidia produced by *F. semitectum* in anthers of *Rudbeckia auriculata* (eared coneflower, Asteraceae) were dispersed by andrenid bees (*Andrena aliciae*). Floral mimicry has been shown to facilitate outcrossing of some self-sterile species of *Puccinia* (Roy, 1993). Because *P. monoica* is heterothallic, pollinating insects are critical for completion of the pathogen life cycle (Roy, 1993; Pfunder and Roy, 2000; Naef et al., 2002). Pollen-collecting bees, butterflies, and flies bring mating-compatible spores of *P. monoica* together when they are attracted to the pseudoflowers by their bright coloration and the sugary and volatile compounds produced by the fungus (Roy, 1993, 1994; Raguso and Roy, 1998). Although sexual reproduction of this rust fungus is facilitated by insects, a role for wind in dispersal of infectious spores that takes place after sexual reproduction was also demonstrated in this system (Roy, 2001). In that regard, in the process of obtaining pure cultures, conidia were dispersed in a visible cloud from a pseudoflower on *X. setigera* when it passed through the air column in a biohood, suggesting that *F. xyrophilum* may also possess a mixed dispersal mode. Unlike the obligate rust *Puccinia*, which has a complex life cycle

involving primary and alternate hosts, fusaria do not require alternate hosts to complete their life cycles.

4.6. Phytohormone gene expression and production

Comparative whole genome analyses of three *F. xyrophilum* strains revealed they have the auxin and cytokinin biosynthetic gene clusters and, therefore, the genetic potential to produce these two classes of phytohormones (Laraba et al., 2019). This genetic potential to synthetize auxin and cytokinin is not exclusive to *F. xyrophilum* and has been documented in several FFSC species (Tsavkelova et al., 2012; Niehaus et al., 2016). The three strains of *F. xyrophilum* shared the same gene expression patterns where auxin and cytokinin biosynthetic genes were expressed in culture, providing further support for the genetic potential of *F. xyrophilum* to produce these phytohormones. CI-GC/MS analysis revealed that the amount of IAA produced was dependent on and enhanced by increasing concentrations of L-tryptophan in the medium. This result is consistent with tryptophan being a precursor of IAA when synthesis occurs via the indole-3-acetamide pathway (Tsavkelova et al., 2012; Niehaus et al., 2016). In addition, the significant differences in the amount of IAA produced by the three strains of *F. xyrophilum* under the same experimental conditions suggests this trait may be strain-specific, as previously reported for *F. proliferatum* (Niehaus et al., 2016). Our data also indicate that the three strains of *F. xyrophilum* synthesized the isoprenoid cytokinin iPR in liquid cultures under the conditions tested, as previously reported for the rice blast fungus, *Magnaporthe oryzae* (Chanclud et al., 2016). Although the role of fungus-derived IAA and cytokinins in plant-fungus interactions is poorly documented, several reports suggest that these hormones may act as virulence factors (Chanclud and Morel, 2016 and references therein). Auxin is a key regulator for many plant growth and developmental processes, including initiation of floral primordia and in specifying the number and identity of floral organs (Cheng and Zhao, 2007). Cano et al. (2013) discovered that genes implicated in diverse mechanisms that control auxin homeostasis were upregulated in *Boechera stricta* pseudoflowers induced by *P. monoica.* These authors speculated that auxin (mainly IAA) might contribute to the remarkable morphology of *B. stricta* pseudoflowers, which are modified leaves, via the maintenance of stem elongation and leaf growth. Accordingly, we hypothesize that the IAA produced by *F. xyrophilum* may prevent the host from switching from the vegetative phase to flowering and inhibit floral organ development. While several studies suggest that auxins and cytokinins might also play a role in several physiological processes in fungi, especially in hyphal development (Chanclud and Morel, 2016), additional research is required to determine whether they are involved in pseudoflower formation and in reprogramming host plant machinery resulting in suppression of flower formation.

5. Conclusion

The present study extends our knowledge of a recently discovered putative floral mimicry system involving the interaction of the fungus *F. xyrophilum* with two species of yellow-eyed grass, *Xyris setigera* and *X. surinamensis*. The system is unique in that the petal-like structures of the resulting pseudoflowers are composed entirely of fungal tissue rather than modified plant tissue as reported for other floral mimicry systems. Based on our data, we hypothesize that this mimicry system evolved to attract insect pollinators, via olfactory and/or visual cues, that facilitate outcrossing of *F. xyrophilum*. Our results provide a firm foundation and mimicry-related hypotheses to test in subsequent field research investigations. If *F. xyrophilum* pseudoflowers are not specifically adapted to the *Xyris* floral signaling system, and only resemble yellow flowers with generic floral cues, then this system would fall under generalized food deception rather than classical Batesian or Müllerian mimicry (Johnson and Schiestl, 2016). Phylogenetic analyses of *Xyris* species and pseudoflower fungi across their range in northern South America are also needed to assess whether host-pathogen associations have been driven by coevolution or host jumps (Roy, 2001), and assess whether only *F. xyrophilum* or a multispecies lineage is involved. Lastly, our study highlights the need for extensive transcriptomic experiments, as reported for *P. monoica* (Cano et al., 2013), to elucidate the biological processes involved in the formation of pseudoflowers so that the diverse floral mimicry systems can be compared directly within an evolutionary genomic framework.

Authors statement

KJW conducted fieldwork and collected the pseudoflowers, IL designed and performed the experiments; MMV, SPM, MB conducted the GC–MS and LC-MS analyses; MA conducted the fluorescence analyses; FF performed the SEM. IL wrote the paper, and all of the authors revised the manuscript.

Acknowledgments

The USDA-ARS National Program for Food Safety and NSF DEB-1655980 provided funding for this study. This research was supported in part by an appointment to the ARS Research Participation Program administered by the Oak Ridge Institute for Science and Education (ORISE) through an interagency agreement between the US Department of Energy (DOE) and the US Department of Agriculture (USDA). ORISE is managed by ORAU under DOE contract number DE-SC0014664. All opinions expressed in this paper are the author's and do not necessarily reflect the policies and views of USDA, DOE, or ORAU/ORISE. Fieldwork by Kenneth J. Wurdack was supported by the National Geographic Society/Waitt Grants Program (Karen Redden, PI) and the Biological Diversity of the Guiana Shield Program (BDG), Smithsonian Institution (SI). The authors wish to thank Mark Strong (SI) for the *Xyris* identifications, E. Keats Webb and Melvin Wachowiak for the UV imaging, which was performed at the SI Museum Conservation Institute, several anonymous reviewers for constructive criticisms on an earlier version of this manuscript, and Amy McGovern and Crystal Probyn for their technical support in generating the whole genome sequence data.

Disclaimer

The mention of company names or trade products does not imply that they are endorsed or recommended by the US Department of Agriculture over other companies or similar products not mentioned. USDA is an equal opportunity provider and employer.

Appendix A. Supplementary material

Supplementary data to this article can be found online at https://doi.org/10.1016/j.fgb.2020.103466.

References

Ajayi, O.E., Balusu, R., Morawo, T.O., Zebelo, S., Fadamiro, H., 2015. Semiochemical modulation of host preference of *Callosobruchus maculatus* on legume seeds. J. Stored Prod. Res. 63, 31–37.

Andersson, S., Nilsson, L.A., Groth, I., Bergström, G., 2002. Floral scents in butterfly-pollinated plants: possible convergence in chemical composition. Bot. J. Linn. Soc. 140, 129–153.

Batra, L.R., Batra, S.W.T., 1985. Floral mimicry induced by mummy-berry fungus exploits host's pollinators as vectors. Science 228, 1011–1013.

Berry, P.E., Riina, R., 2005. Insights into the diversity of the Pantepui flora and the biogeographic complexity of the Guayana Shield. Biol. Skr. 5, 145–167.

Blight, M.M., Le Metayer, M., Delegue, M.H.P., Pickett, J.A., Marion-Poll, F., Wadhams, L.J., 1997. Identification of floral volatiles involved in recognition of oilseed rape flowers, *Brassica napus* by honeybees, *Apis mellifera*. J. Chem. Ecol. 23, 1715–1727.

Boyd, R.S., Teem, A., Wall, M.A., 2011. Floral biology of an Alabama population of the federally endangered plant, *Xyris tennesseensis* Kral (Xyridaceae). Castanea 76, 255–265.

Briscoe, A.D., Chittka, L., 2001. The evolution of color vision in insects. Annu. Rev. Entomol. 46, 471–510.

Busman, M., 2017. Utilization of high performance liquid chromatography coupled to tandem mass spectrometry for characterization of *8-O*-methylbostrycoidin production by species of the fungus *Fusarium*. J. Fungi 3, 43.
Campbell, L.M., 2011. *Xyris bracteicaulis*, a new species from the coastal plain of New York. Harv. Pap. Bot. 16, 49–51.
Cano, L.M., Raffaele, S., Haugen, R.H., Saunders, D.G.O., Leonelli, L., MacLean, D., Hogenhout, S.A., Kamoun, S., 2013. Major transcriptome reprogramming underlies floral mimicry induced by the rust fungus *Puccinia monoica* in *Boechera stricta*. PLoS ONE 8 (9), e75293. https://doi.org/10.1371/journal.pone.0075293.
Chanclud, E., Kisiala, A., Emery, N.R.J., Chalvon, V., Ducasse, A., Romiti-Michel, C., Gravot, A., Kroj, T., Morel, J.B., 2016. Cytokinin production by the rice blast fungus is a pivotal requirement for full virulence. PLoS Pathog. 12 (2), e1005457 https://doi.org/10.1371/journal.ppat.1005457.
Chanclud, E., Morel, J.B., 2016. Plant hormones: a fungal point of view. Mol. Plant Pathol. 17, 1289–1297.
Chen, G., Su, Q., Shi, X., Liu, X., Peng, Z., Zheng, H., Xie, W., Xu, B., Wang, S., Wu, Q., Zhou, X., Zhang, Y., 2017. Odor, not performance, dictates *Bemisia tabaci*'s selection between healthy and virus infected plants. Front. Physiol. 8, 146. https://doi.org/10.3389/fphys.2017.00146.
Cheng, Y., Zhao, Y., 2007. A role for auxin in flower development. J. Integr. Plant Biol. 49, 99–104.
Dafoe, N.J., Thomas, J.D., Shirk, P.D., Legaspi, M.E., Vaughan, M.M., Huffaker, A., Teal, P.E., Schmelz, E.A., 2013. European corn borer (*Ostrinia nubilalis*) induced responses enhance susceptibility in maize. PLoS ONE 8 (9), e73394.
Diamond, A.R., El Mayas, H., Boyd, R.S., 2006. *Rudbeckia auriculata* infected with a pollen- mimic fungus in Alabama. Southeast. Nat. 5, 103–112.
Edgar, R.C., 2004. MUSCLE: multiple sequence alignment with high accuracy and high throughput. Nucleic Acids Res. 32, 1792–1797.
Eisner, T., 2002. An insect's view of a flower. Am. Entomol. 48, 142–143.
El-Sayed, A.M., Unelius, C.R., Suckling, D.M., 2018. Honey norisoprenoids attract bumble bee, *Bombus terrestris*, in New Zealand mountain beech forests. J. Agric, Food Chem. 66, 13065–13072.
Gouy, M., Guindon, S., Gascuel, O., 2010. SeaView version 4: a multiplatform graphical user interface for sequence alignment and phylogenetic tree building. Mol. Bio. Evol. 27, 221–224.
Grajales-Conesa, J., Meléndez Ramírez, V., Cruz-López, L., Sánchez Guillén, D., 2012. Effect of citrus floral extracts on the foraging behavior of the stingless bee *Scaptotrigona pectoralis*. Rev. Bras. Entomol. 56, 76–80.
Haverkamp, A., Hansson, B.S., Knaden, M., 2018. Combinatorial codes and labeled lines: how insects use olfactory cues to find and judge food, mates, and oviposition sites in complex environments. Front. Physiol. 9, 49. https://doi.org/10.3389/fphys.2018.00049.
Hawksworth, D.L., Lücking, R., 2017. Fungal diversity revisited: 2.2 to 3.8 million species. Microbiol. Spectr. 5 https://doi.org/10.1128/microbiolspec.FUNK-0052-2016.
Hills, H.G., Williams, N.H., Dodson, C.H., 1972. Floral fragrances and isolating mechanisms in the genus *Catasetum* (Orchidaceae). Biotropica 4, 61–76.
Huffaker, A., Kaplan, F., Vaughan, M.M., Dafoe, N.J., Ni, X., Rocca, J.R., Alborn, H.T., Teal, P.E.A., Schmelz, E.A., 2011. Novel acidic sesquiterpenoids constitute a dominant class of pathogen-induced phytoalexins in maize. Plant Physiol. 156, 2082–2097.
Hughes, T.J., O'Donnell, K., Sink, S., Rooney, A.P., Scandiani, M.M., Luque, A., Bhattacharyya, M.K., Huang, X., 2014. Architecture and evolution of the mating type locus in fusaria that cause soybean sudden death syndrome and bean root rot. Mycologia 106, 686–697.
Jakobsen, H.B., Kristjánsson, K., Rohde, B., Terkildsen, M., Olsen, C.E., 1995. Can social bees be influenced to choose a specific feeding station by adding the scent of the station to the hive air? J. Chem. Ecol. 21, 1635–1648.
James, D.G., 2005. Further field evaluation of synthetic herbivore induced plant volatiles as attractants for beneficial insects. J. Chem. Ecol. 31, 481–495.
Johnson, S.D., Schiestl, F.P., 2016. Floral Mimicry. Oxford University Press, United Kingdom.
Kerényi, Z., Moretti, A., Waalwijk, C., Oláh, B., Hornok, L., 2004. Mating type sequences in asexually reproducing *Fusarium* species. Appl. Environ. Microbiol. 70, 4419–4423.
Kirk, P.M., Cannon, P.F., Minter, D.W., Stalpers, J.A., 2008. Ainsworth and Bisby's dictionary of the fungi. CAB International, Wallingford.
Kral, R., 1966. The genus *Xyris* (Xyridaceae) in the southeastern United States and Canada. SIDA Contrib. Bot. 2, 177–260.
Kral, R., 1988. The genus *Xyris* (Xyridaceae) in Venezuela and contiguous northern South America. Ann. Mo. Bot. Gard. 75, 522–572.
Landolt, P.J., Adams, T., Zack, R.S., Crabo, L., 2011. A diversity of moths (Lepidoptera) trapped with two feeding attractants. Ann. Entomol. Soc. Am. 104, 498–506.
Laraba, I., Boureghda, H., Abdallah, N., Bouaicha, O., Obanor, F., Moretti, A., Geiser, D. M., Kim, H.-S., McCormick, S.P., Proctor, R.H., et al., 2017. Population genetic structure and mycotoxin potential of the wheat crown rot and head blight pathogen *Fusarium culmorum* in Algeria. Fungal Genet. Biol. 103, 34–41.
Laraba, I., Keddad, A., Boureghda, H., Abdallah, N., Vaughan, M.M., Proctor, R.H., Busman, M., O'Donnell, K., 2018. *Fusarium algeriense*, sp. nov., a novel toxigenic crown rot pathogen of durum wheat from Algeria is nested in the *Fusarium burgessii* species complex. Mycologia 109, 935–950.
Laraba, I., Kim, H.-S., Proctor, R.H., Busman, M., O'Donnell, K., Felker, F.C., Aime, M.C., Koch, R.A., Wurdack, K.J., 2019. Fusarium xyrophilum, sp. nov., a member of the Fusarium fujikuroi species complex recovered from pseudoflowers on yellow-eyed grass (Xyris spp.) from Guyana. Mycologia. doi: 10.1080/00275514.2019.1668991.
Lee, K., Pan, J.J., May, G., 2009. Endophytic *Fusarium verticillioides* reduces disease severity caused by *Ustilago maydis* on maize. FEMS Microbiol. Lett. 299, 31–37.
Lofgren, L.A., LeBlanc, N.R., Certano, A.K., Nachtigall, J., LaBine, K.M., Riddle, J., Broz, K., Dong, Y., Bethan, B., Kafer, C.W., et al., 2018. *Fusarium graminearum*: pathogen or endophyte of North American grasses? New Phytol. 217, 1203–1212.
Martin, S.H., Wingfield, B.D., Wingfield, M.J., Steenkamp, E.T., 2011. Structure and evolution of the *Fusarium* mating type locus: new insights from the *Gibberella fujikuroi* complex. Fungal Genet. Biol. 48, 731–740.
Mazza, C.A., Izaguirre, M.M., Curiale, J., Ballaré, C.L., 2010. A look into the invisible: ultraviolet-B sensitivity in an insect (*Caliothrips phaseali*) revealed through a behavioural action spectrum. Pro. R. Soc. B 277, 367–373.
McArt, S.H., Miles, T.D., Rodriguez-Saona, C., Schilder, A., Adler, L.S., Grieshop, M.J., 2016. Floral scent mimicry and vector-pathogen associations in a pseudoflower-inducing plant pathogen system. PLoS ONE 11 (11), e0165761.
Miller, J.D., Greenhalgh, R., 1985. Nutrient effects on the biosynthesis of trichothecenes and other metabolites by *Fusarium graminearum*. Mycologia 77, 130–136.
Murai, T., Imai, T., Maekawa, M., 2000. Methyl anthranilate as an attractant for two thrips species and the thrips parasitoid *Ceranisus menes*. J. Chem. Ecol. 26, 2557–2565.
Naef, A., Roy, B.A., Kaiser, R., Honegger, R., 2002. Insect-mediated reproduction of systemic infections by *Puccinia arrhenatheri* on *Berberis vulgaris*. New Phytol. 154, 717–730.
Ngugi, H.K., Scherm, H., 2006. Mimicry in plant-parasitic fungi. FEMS Microbiol. Lett. 257, 171–176.
Nguyen, L.-T., Schmidt, H.A., von Haeseler, A., Minh, B.Q., 2015. IQ-TREE: a fast and effective stochastic algorithm for estimating maximum likelihood phylogenies. Mol. Biol. Evol. 32, 268–274. https://doi.org/10.1093/molbev/msu300.
Niehaus, E.M., Munsterkotter, M., Proctor, R.H., Brown, D.W., Sharon, A., Idan, Y., Oren-Young, L., Sieber, C.M., Novak, O., Pencik, A., et al., 2016. Comparative "Omics" of the *Fusarium fujikuroi* species complex highlights differences in genetic potential and metabolite synthesis. Genome Biol. Evol. 8, 3574–3599.
O'Donnell, K., Rooney, A.P., Proctor, R.H., Brown, D.W., McCormick, S.P., Ward, T.J., Frandsen, R.J.N., Lysøe, E., Rehner, S.A., Aoki, T., et al., 2013. Phylogenetic analyses of *RPB1* and *RPB2* support a middle Cretaceous origin for a clade comprising all agriculturally and medically important fusaria. Fungal Genet. Biol. 52, 20–31.
O'Donnell, K., Sutton, D.A., Rinaldi, M.G., Gueidan, C., Sarver, B.A.J., Balajee, S.A., Schroers, H.-J., Summerbell, R.C., Robert, V.A.R.G., Crous, P.W., et al., 2010. Internet-accessible DNA sequence database for identifying fusaria from human and animal infections. J. Clin. Microbiol. 48, 3708–3718.
Ostroverkhova, O., Galindo, G., Lande, C., Kirby, J., Scherr, M., Hoffman, G., Rao, S., 2018. Understanding innate preferences of wild bee species: responses to wavelength-dependent selective excitation of blue and green photoreceptor types. J. Comp. Physiol. A 204, 667–675.
Peitsch, D., Fietz, A., Hertel, H., de Souza, J., Ventura, D.F., Menzel, R., 1992. The spectral input systems of hymenopteran insects and their receptor-based colour vision. J. Comp. Physiol. A 170, 23–40.
Pfunder, M., Roy, B.A., 2000. Pollinator-mediated interactions between a pathogenic fungus, *Uromyces pisi* (Pucciniaceae), and its host plant, *Euphorbia cyparissias* (Euphorbiaceae). Am. J. Bot. 87, 48–55.
Raguso, R.A., Roy, B.A., 1998. 'Floral' scent production by *Puccinia* rust fungi that mimic flowers. Mol. Ecol. 7, 1127–1136.
Ramirez, N., 1993. Reproductive biology in a tropical shrubland of Venezuelan Guayana. J. Veg. Sci. 4, 5–12.
Rao, S., Ostroverkhova, O., 2015. Visual outdoor response of multiple wild bee species: highly selective stimulation of a single photoreceptor type by sunlight-induced fluorescence. J. Com. Physiol. A 201, 705–716.
Rering, C.C., Beck, J.J., Hall, G.W., McCartney, M.M., Vannette, R.L., 2018. Nectar-inhabiting microorganisms influence nectar volatile composition and attractiveness to a generalist pollinator. New Phytol. 220, 750–759.
Roy, B.A., 1993. Floral mimicry by a plant pathogen. Nature 362, 56–58.
Roy, B.A., 1994. The use and abuse of pollinators by fungi. Trends Ecol. Evol. 9, 335–339.
Roy, B.A., 1996. A plant pathogen influences pollinator behavior and may influence reproduction of nonhosts. Ecology 77, 2445–2457.
Roy, B.A., 2001. Patterns of association between crucifers and their flower-mimic pathogens: host jumps are more common than coevolution or cospeciation. Evolution 55, 41–53.
Sauquet, H., von Balthazar, M., Magallón, S., Doyle, J.A., Endress, P.K., Bailes, E.J., de Morais, E.B., Bull-Hereñu, K., Carrive, L., Chartier, M., et al., 2017. The ancestral flower of angiosperms and its early diversification. Nature Commun. 8, 16047. https://doi.org/10.1038/ncomms16047.
Schaeffer, R.N., Rering, C.C., Maalouf, I., Beck, J.J., Vannette, R.L., 2019. Microbial metabolites elicit distinct olfactory and gustatory preferences in bumblebees. Biol. Lett. 15, 20190132. https://doi.org/10.1098/rsbl.2019.0132.
Schmelz, E.A., Engelberth, J., Tumlinson, J.H., Block, A., Alborn, H.T., 2004. The use of vapor phase extraction in metabolic profiling of phytohormones and other metabolites. Plant J. 39, 790–808.
Shinners, T.C., Olson, A.R., 1996. The gynoecial infection pathway of *Monilinia vaccinii-corymbosi* in lowbush blueberry (*Vaccinium angustifolium*). Can. J. Plant Sci. 76, 493–497.
Stanke, M., Steinkamp, R., Waack, S., Morgenstern, B., 2004. AUGUSTUS: A web server for gene finding in eukaryotes. Nucleic Acids Res. 32, W309–W312. https://doi.org/10.1093/nar/gkh379.
Stevens, R.B., 1974. Mycology guidebook. University of Washington Press, Seattle.

Studt, L., Wiemann, P., Kleigrewe, K., Humpf, H.U., Tudzynski, B., 2012. Biosynthesis of fusarubins accounts for pigmentation of *Fusarium fujikuroi* perithecia. Appl. Environ. Microbiol. 78, 4468–4480.

Summerell, B.A., 2019. Resolving *Fusarium*: current status of the genus. Annu. Rev. Phytopathol. 57, 323–339.

Svensson, B.G., Bergström, G., 1977. Volatile marking secretions from the labial gland of North European *Pyrobombus* D. T. males (Hymenoptera, Apidae). Insectes Soc. 24, 213–224.

Tholl, D., Boland, W., Hansel, A., Loreto, F., Röse, U.S.R., Schnitzler, J.P., 2006. Practical approaches to plant volatile analysis. Plant J. 45, 540–560.

Tsavkelova, E., Oeser, B., Oren-Young, L., Israeli, M., Sasson, Y., Tudzynski, B., Sharon, A., 2012. Identification and functional characterization of indole-3-acetamide-mediated IAA biosynthesis in plant-associated *Fusarium* species. Fungal Genet. Biol. 49, 48–57.

Twidle, A.M., Mas, F., Harper, A.R., Horner, R.M., Welsh, T.J., Suckling, D.M., 2015. Kiwifruit flower odor perception and recognition by honey bees, *Apis mellifera*. J. Agric. Food Chem. 63, 5597–5602.

Valterová, I., Kunze, J., Gumbert, A., Luxová, A., Liblikas, I., Kalinová, B., Borg-Karlson, A.K., 2007. Male bumble bee pheromonal components in the scent of deceit pollinated orchids; unrecognized pollinator cues? Arthropod-Plant Inte. 1, 137–145.

Yun, S.H., Arie, T., Kaneko, I., Yoder, O.C., Turgeon, B.G., 2000. Molecular organization of mating type loci in heterothallic, homothallic, and asexual *Gibberella/Fusarium* species. Fungal Genet. Biol. 31, 7–20.

Zhou, X., O'Donnell, K., Kim, H.-S., Proctor, R.H., Doehring, G., Cao, Z.-M., 2018. Heterothallic sexual reproduction in three canker-inducing tree pathogens within the *Fusarium torreyae* species complex. Mycologia 110, 710–725.